Do Southern Hemisphere tree rings record past volcanic events?

Philippa A. Higgins[1,2], Jonathan G. Palmer[2,3], Chris S. M. Turney[2,3], Martin S. Andersen[4], Fiona Johnson[1]

[1]Water Research Centre, School of Civil and Environmental Engineering, UNSW Sydney, NSW, 2052, Australia
[2]ARC Centre of Excellence for Australian Biodiversity and Heritage, University of New South Wales, NSW 2052, Australia
[3]Earth and Sustainability Science Research Centre, School of Biological, Earth and Environmental Sciences, University of New South Wales, NSW 2052, Australia
[4]Water Research Laboratory, School of Civil & Environmental Engineering, UNSW Sydney, NSW 2052, Australia

Table S1 – Details of volcanic eruptions between 1400 and 1990 CE selected using the two thresholds of modelled SAOD over New Zealand (> 0.04 or > 0.08), and prior and secondary eruptions with SAOD > 0.01. Eruptions within 5 years prior of the target eruption were removed and the baseline period selected as the closest non-volcanically disturbed period. Secondary eruptions occurring within 5 years of the target eruption were also removed prior to averaging the SEA ensemble (Büntgen et al., 2020).

Eruption date (month/year)	Eruption	Locality	Latitude	SAOD threshold	Prior Eruption	Secondary Eruption
1452	Kuwae	Vanuatu	16.8°S	> 0.04	1448 (-4)	1457 (+5)
1457	Unknown			> 0.08	1452 (-5)	
2/1477	Bárðarbunga	Iceland	64.6°N	> 0.04		
1595	Unknown			> 0.08	1590 (-5)	1600 (+5)
2/1600	Huaynaputina	Peru	16.6°S	> 0.08	1595 (-5)	
1620	Unknown			> 0.04		
†12/1640	Parker	Philippines	6.1°N	> 0.08		
1653	Unknown			> 0.04		
1673	Gamnokara	Japan	1.4°N	> 0.04		
1694	Unknown			> 0.08		
1761	Unknown			> 0.04		
5/1783	Grímsvötn	Iceland	64.4°N	> 0.08		
	Asama	Japan	36.4°N			
1809	Unknown			> 0.08		
4/1815	Tambora	Sundas	8.3°S	> 0.08		
1831	Babuyan Claro*	Philippines	19.5°N	> 0.04		1835 (+4)
1/1835	Cosigüina	Nicaragua	13.0°N	> 0.08	1831 (-4)	
†12/1861	Makian		0.3°N	> 0.04		
8/1883	Krakatau	Indonesia	6.1°S	> 0.08		1886 (+3)
10/1902	Santa Maria	Guatemala	14.8°N	not modelled		
3/1963	Agung	Bali	8.3°S	not modelled		
3/1982	El Chicon	México	17.4°N	not modelled		

†Eruptions occurring in December were assigned an eruption year of year+1 in the superposed epoch analysis event list for consistency with the designation of years in the temperature reconstruction (reconstruction year 1641 is Dec 1640 – Feb 1641).

* Location is disputed (Garrison et al., 2018).

Table S2 – Coupled Model Intercomparison Project 5 (CMIP5) models used in the analysis.

Model	No. of Ens.	Solar	Volcanic	GHG	Land Use	Reference
GISS-E2-R 121	1	Steinhilber et al	Crowley & Unterman (2013)	Schmidt et al. (2012)	Pongratz et al. (2008)	Schmidt et al. (2014)
GISS-E2-R 124	1	Viera et al. (2011)	Crowley & Unterman (2013)	Schmidt et al. (2012)	Pongratz et al. (2008)	Schmidt et al. (2014)
GISS-E2-R 127	1	Viera et al. (2011)	Crowley & Unterman (2013)	Schmidt et al. (2012)	Kaplan et al. (2010)	Schmidt et al. (2014)
FGOALS-gl	1	Crowley (2000)	Crowley (2000)	Amman et al. (2007)	-	Guo and Zhou (2013)
MRI-CGCM3	1	Delaygue & Bard (2011) + Wang et al. (2005)	Gao et al. (2008)	Schmidt et al. (2012)	-	Yukimoto et al. (2012)
MPI-ESM-P	3	Viera et al. (2011)	Crowley & Unterman (2013)	Schmidt et al. (2012)	Pongratz et al. (2008)	Jungclaus et al. (2014)
MIROC-ESM	1	Delaygue & Bard (2011) + Wang et al. (2005)	Crowley et al. (2008)	Schmidt et al. (2012)	-	Sueyoshi et al. (2013)

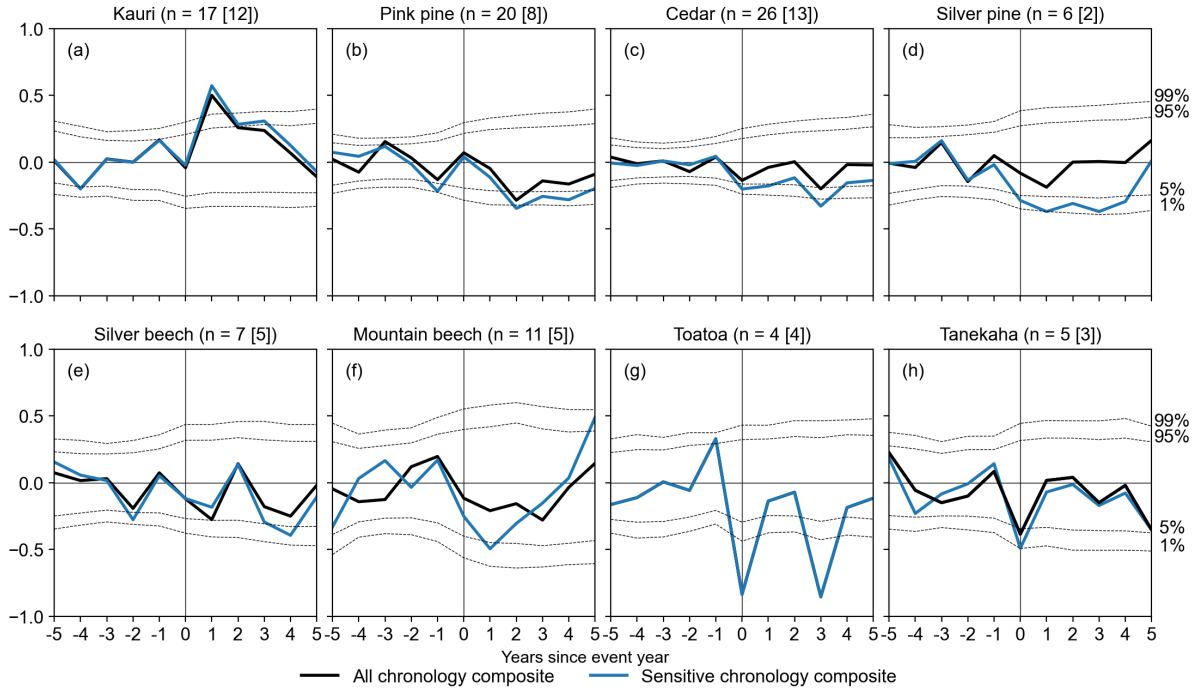

Figure S1 – Mean chronology departures five years before and after 21 eruption years with SAOD > 0.04 (year 0), separated by tree species. The number of chronologies contributing to the species-wide composite (black) and the sensitive chronology composite (blue) and are shown in brackets/square brackets. Significance bands are the 1st, 5th, 95th, and 99th percentile of 10,000 block reshuffled replicates of the species wide response.

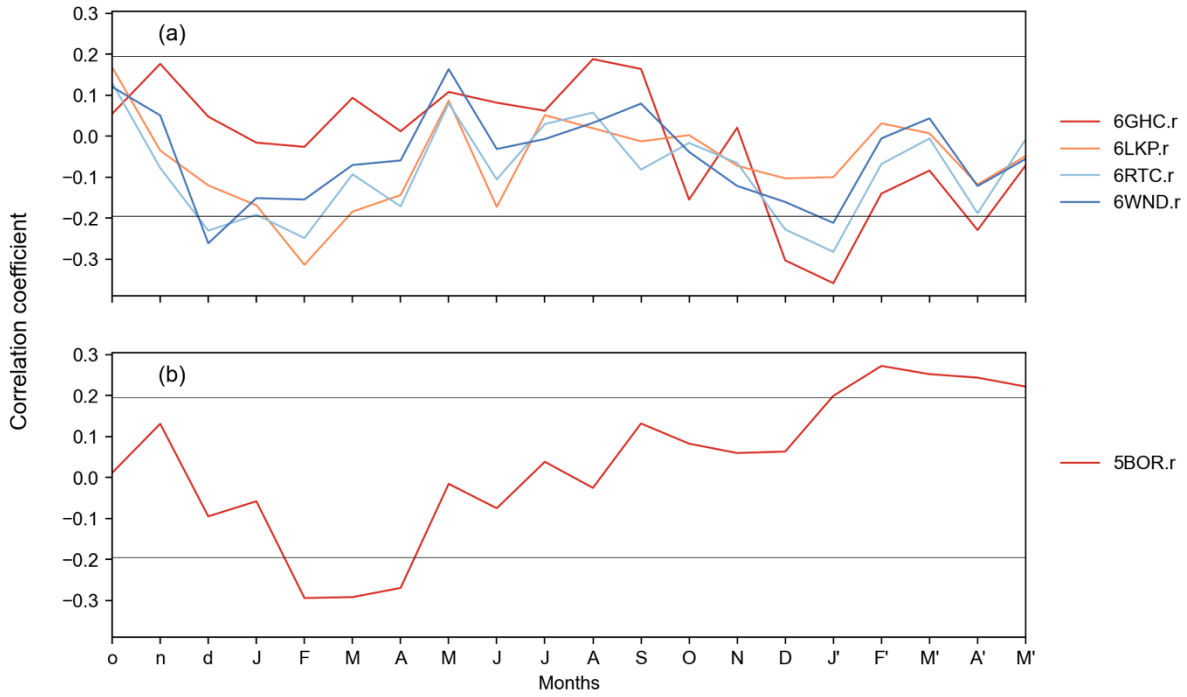

Figure S2– Correlation between beech ring widths and monthly New Zealand seven-station average monthly temperature from 1911–1990 for the 20-month window extending from October of the previous growing season to May at the end of the current austral growing season: a) Mountain beech (*Fuscopora cliffortioides*) and b) Silver beech (*Lophozonia menziesii*). Horizontal lines indicate the threshold for significance at $p < 0.05$.

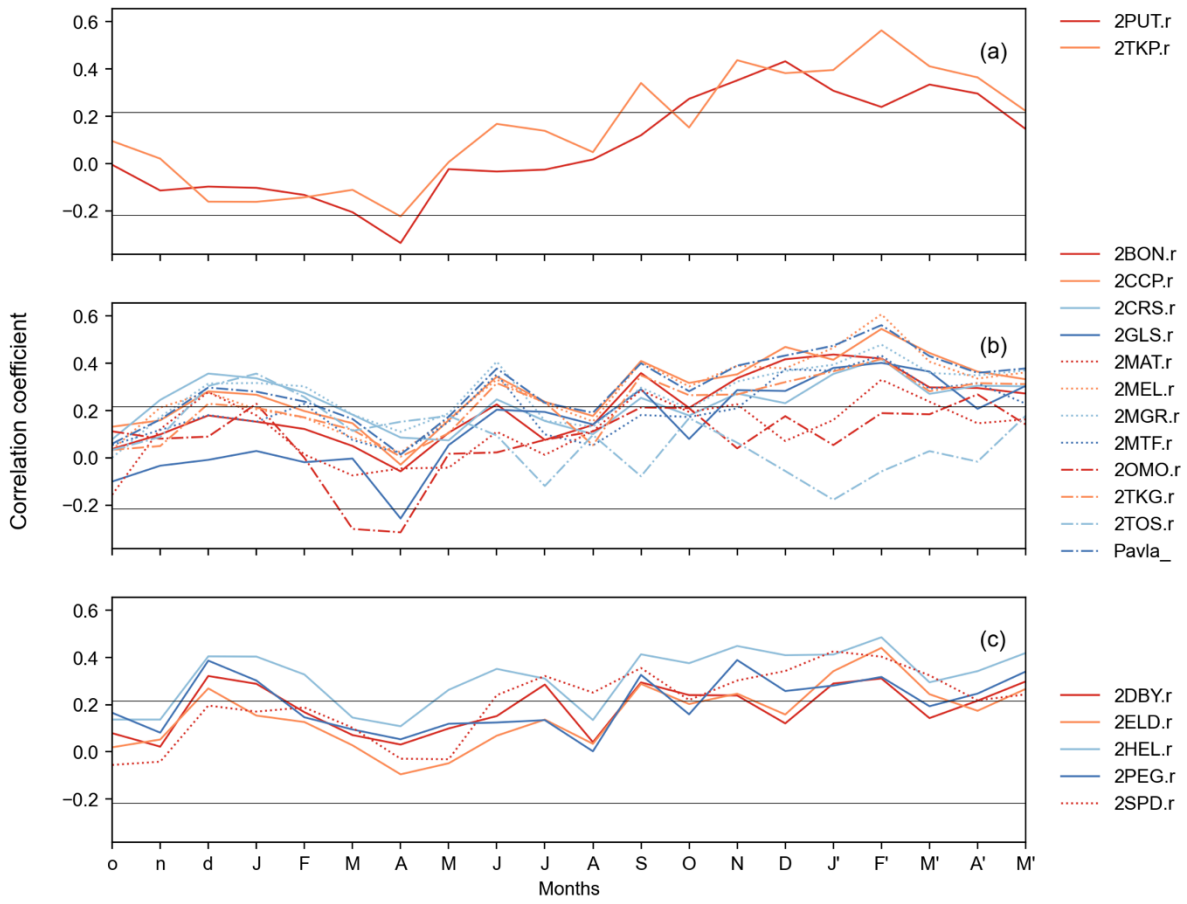

Figure S3 – Correlation between pink pine (*Halocarpus biformis*) ring widths and monthly New Zealand seven-station average monthly temperature from 1911 – 1990 for the 20-month window extending from October of the previous growing season to May at the end of the current austral growing season: a) Chronologies from the North Island, b) Chronologies from the western coast of the South Island, c) Chronologies south of latitude -45° on the South Island. Pavla_ is the Pink Pine master chronology. Horizontal lines indicate the threshold for significance at $p < 0.05$

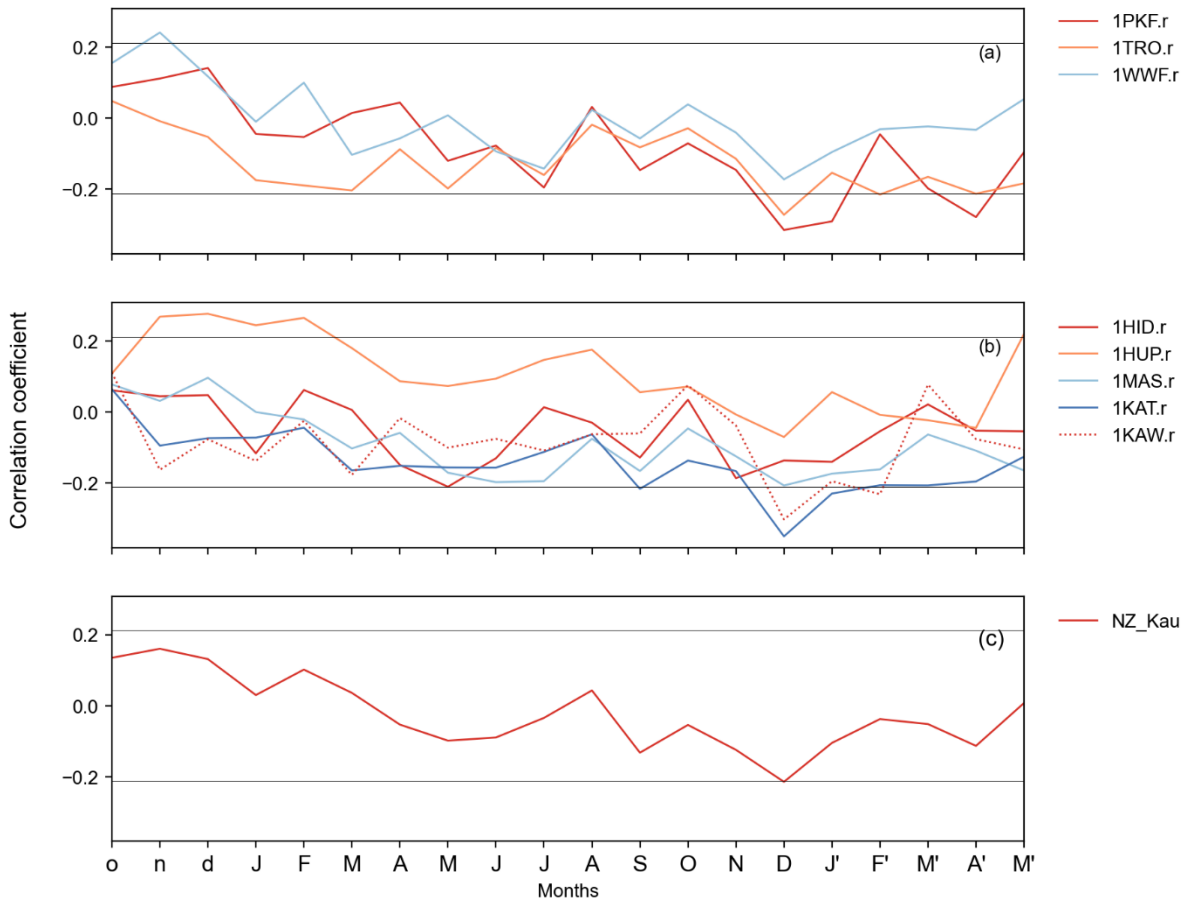

Figure S4 – Correlation between kauri (*Agathis australis*) ring widths and monthly New Zealand seven-station average monthly temperature from 1911 – 1990 for the 20-month window extending from October of the previous growing season to May at the end of the current austral growing season: a) Chronologies north of latitude -36° on the North Island, b) Chronologies south of -36° latitude c) Kauri master chronology. Horizontal lines indicate the threshold for significance at $p < 0.05$.

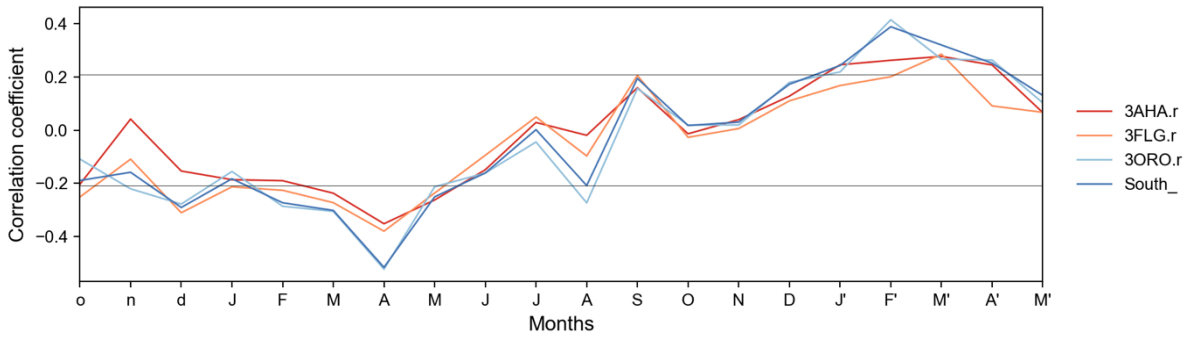

Figure S5 – Correlation between silver pine (*Manoao colensoi*) ring widths and monthly New Zealand seven-station average monthly temperature from 1911 – 1990 for the 20-month window extending from October of the previous growing season to May at the end of the current austral growing season. South_ is the master chronology. Horizontal lines indicate the threshold for significance at $p < 0.05$.

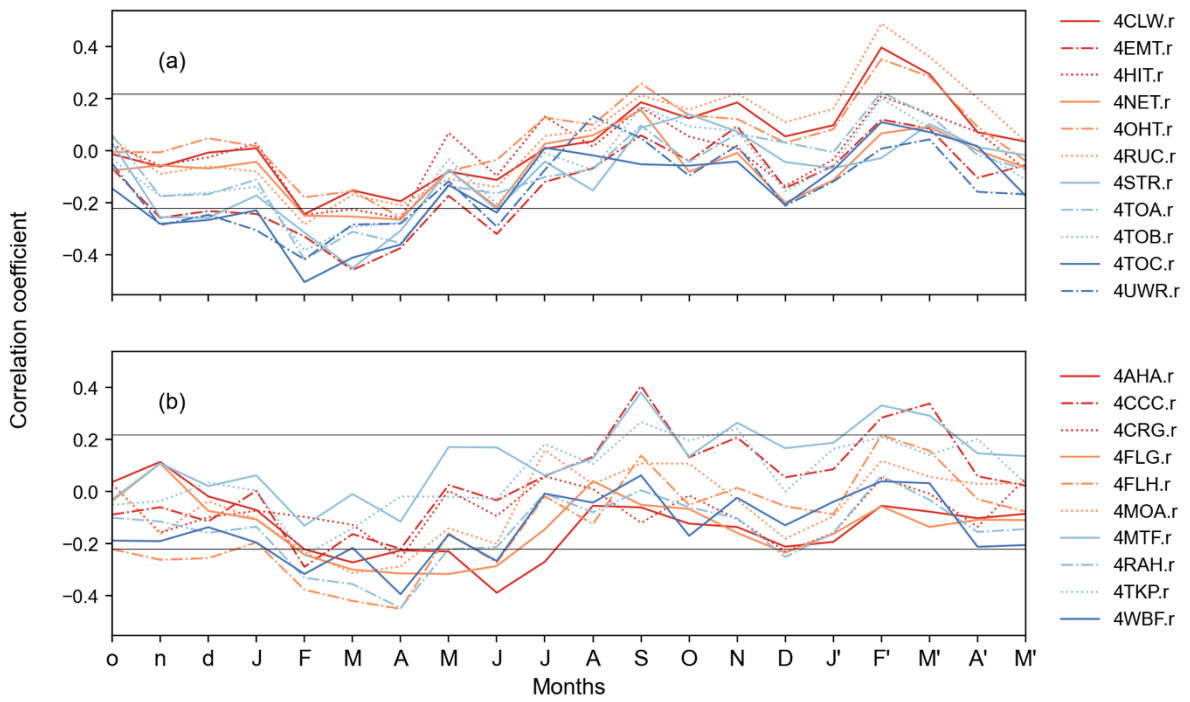

Figure S6– Correlation between cedar (*Libocedrus bidwillii*) ring widths and monthly New Zealand seven-station average monthly temperature from 1911 – 1990 for the 20-month window extending from October of the previous growing season to May at the end of the current austral growing season: a) Chronologies from the North Island, b) Chronologies from the South Island. Horizontal lines indicate the threshold for significance at $p < 0.05$.

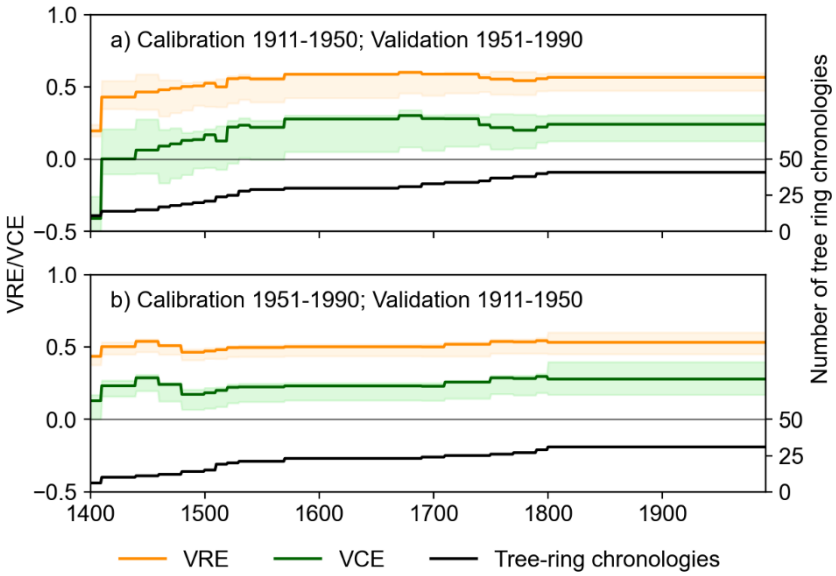

Figure S7 – Verification statistics for the NZall temperature reconstruction a) using the early calibration window and b) using the late calibration window. The 90% uncertainty interval around the verification period reduction of error (VRE; orange) and verification period coefficient of efficiency (VCE; green) were calculated from 300 maximum entropy bootstrap replications. The secondary axis shows the number of tree-ring chronologies contributing to the reconstruction over time.

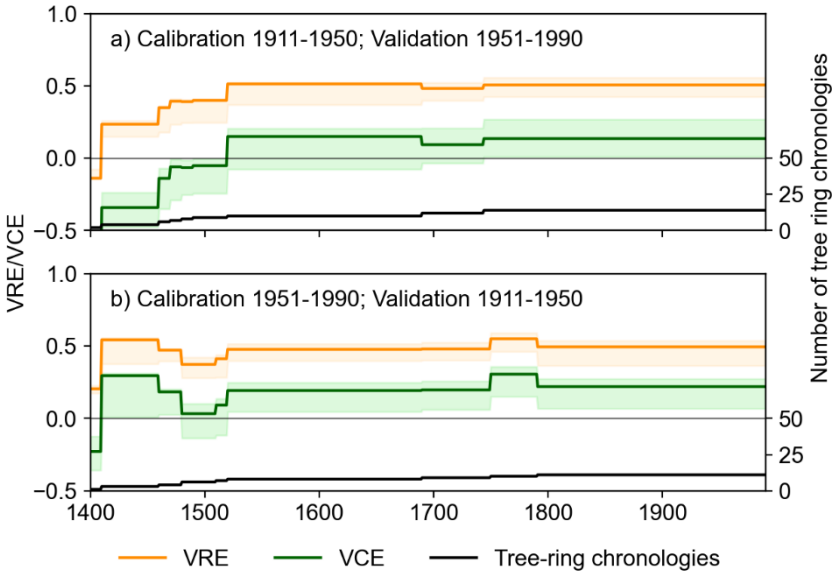

Figure S8 – Verification statistics for the NZsens temperature reconstruction a) using the early calibration window and b) using the late calibration window. The 90% uncertainty interval around the verification period reduction of error (VRE; orange) and verification period coefficient of efficiency (VCE; green) were calculated from 300 maximum entropy bootstrap replications. The secondary axis shows the number of tree-ring chronologies contributing to the reconstruction over time.

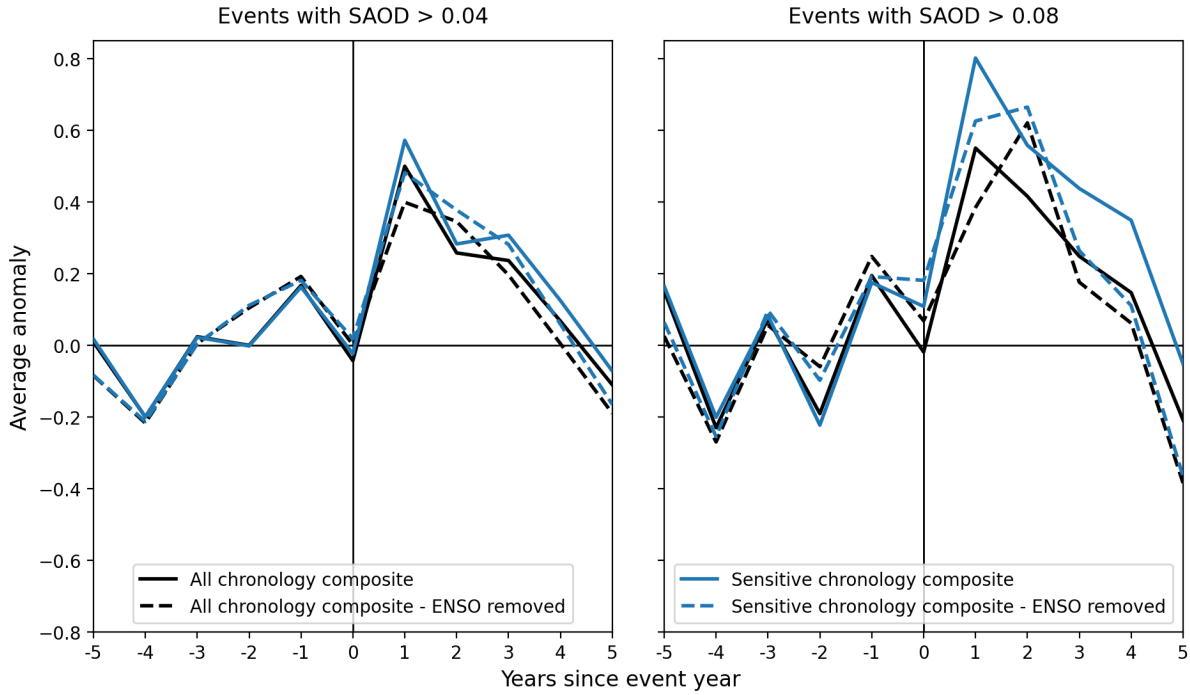

Figure S9 – Impact of removing volcanic events occurring simultaneously with a known El Niño event (1902, 1963, and 1982) from the key event list on the SEA results for kauri. All results are significant in year t+1 except for the 'All chronology composite' for the events with SAOD > 0.08 after the known El Niño events are removed (n = 10). For this series, only the t+2 anomaly is significant.

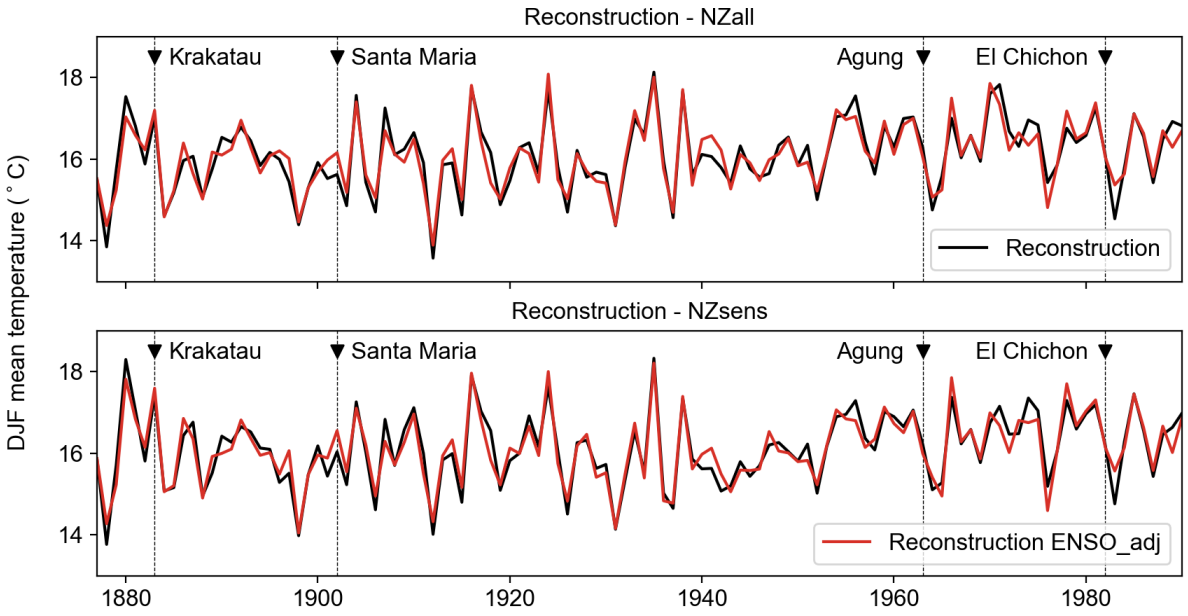

Figure S10 – Reconstructed temperatures in black and the same data with ENSO removed in red. The four large volcanic eruptions occurring during the period for which instrumental ENSO indices are available (Southern Oscillation Index; 1778 CE to present) are also shown.